

Nonmonotonic thickness dependence of spin wave energy in ultrathin Fe films: Experiment and theory

Y. Zhang (张雨),¹ P. Buczek,¹ L. Sandratskii,¹ W. X. Tang (唐文新),^{1,2,*} J. Prokop,¹ I. Tudosa,¹ T. R. F. Peixoto,^{1,3} Kh. Zakeri,¹ and J. Kirschner¹

¹Max-Planck-Institut für Mikrostrukturphysik, Weinberg 2, 06120 Halle, Germany

²School of Physics, Monash University, Victoria 3800, Australia

³Instituto de Física, Universidade de São Paulo, São Paulo 05508-090, SP, Brazil

(Received 5 March 2010; published 31 March 2010)

High wave-vector spin waves in ultrathin Fe/W(110) films up to 20 monolayers (MLs) thick have been studied using spin-polarized electron energy-loss spectroscopy. An unusual nonmonotonous dependence of the spin wave energies on the film thickness is observed, featuring a pronounced maximum at 2 ML coverage. First-principles theoretical study reveals the origin of this behavior to be in the localization of the spin waves at the surface of the film, as well as in the properties of the interlayer exchange coupling influenced by the hybridization of the electron states of the film and substrate and by the strain.

DOI: [10.1103/PhysRevB.81.094438](https://doi.org/10.1103/PhysRevB.81.094438)

PACS number(s): 75.30.Ds, 75.50.Bb, 75.70.Ak

I. INTRODUCTION

Understanding of the elementary magnetic excitation such as spin waves (SWs) in ferromagnets, and the processes governing the spin dynamics on the atomic length (10^{-10} m) and femtosecond time scale (10^{-15} s), is one of the challenging topics in modern solid-state physics.¹ In particular, exploring high wave-vector SWs in low-dimensional magnets and their response to the reduced dimensionality, hybridization effects and strain, is essential to understand the intrinsic properties such as microscopic exchange interaction, magnetic ordering, and spin dynamics. Besides those core physical properties, high-energy SWs are also linked with phenomena such as fast magnetization reversal, polarized current induced magnetization switching, and domain-wall motion. This knowledge is crucial for designing faster and smaller spintronic devices.² Recent experiments indicate that the coupling between electrons and high-energy SWs is a possible coupling mechanism leading to high-temperature superconductivity.^{3,4}

Bulk SWs can be studied by means of inelastic neutron scattering^{5,6} but the method cannot be applied to ultrathin films because it lacks surface sensitivity. SWs in thin films and on the surface can be probed by ferromagnetic resonance and Brillouin light scattering^{1,7} but those techniques are limited in a very small wave-vector region around the Brillouin-zone center. Recently, inelastic scanning tunneling spectroscopy^{8,9} has been used to excite standing SWs in magnetic thin films but the method does not provide in-plane momentum resolution. Up to now, only the spin-polarized electron energy-loss spectroscopy (SPEELS) (Refs. 10–13) is capable of probing high-energy genuine surface SWs across the whole surface Brillouin zone. The applicability of SPEELS has been firmly established by mapping the SW dispersion relation in 1- and 2-monolayer (ML)-thick Fe/W(110) films.^{14,15} Combined with first-principles theoretical approaches SPEELS can help to refine microscopic models of nanomagnets.^{16–18}

In this work we present an experimental attempt to determine directly and systematically the properties of high-energy SWs in ferromagnetic Fe thin films of varying thickness. We discover that for the investigated in-plane momentum transfers \mathbf{q} between 0.5 and 0.7 \AA^{-1} the energy of SWs, $\omega_n(\mathbf{q})$, is a nonmonotonous function of the thickness n (expressed in ML), with a distinct maximum for a 2-ML-thick film. An accompanying first-principles theoretical study of the SW excitations uses the clear experimental trend to choose between two complementary scenarios of polarized electron scattering. The theory suggests that the SWs excited in the experiment are localized at the surface of the film. Both the hybridization with substrate and the atomic relaxation of the Fe film are important for the nonmonotonous behavior of the SW energy.

This paper is structured as follows: In Sec. II we introduce the experiments on preparation, characterization, and SPEELS measurements of the Fe thin films on W(110). In Sec. III we present the experimental and theoretical results focusing the discussion on the nonmonotonous thickness dependence of the spin wave energies. The conclusions will be finally given in Sec. IV.

II. EXPERIMENT

The experiments were performed in an ultrahigh vacuum chamber with a base pressure below 5×10^{-11} mbar. The ultrathin Fe films, with thickness between 1 and 20 ML were prepared by molecular-beam epitaxy at room temperature. After the deposition of Fe, the samples underwent a slight annealing in order to improve the structural quality.¹⁹ The thickness uncertainty was well below 10%. Subsequently, the hysteresis loops of the films were recorded by the magneto-optic Kerr effect (MOKE) measurements in the longitudinal geometry. In the MOKE measurements the magnetic field was applied along the in-plane [110] direction.

The SPEEL spectra were measured in the magnetic remanent state using a high-performance SPEEL spectrometer.^{10–15} The total-energy resolution was between

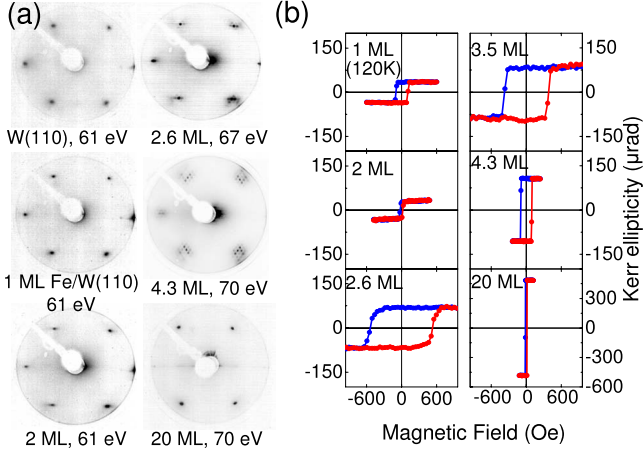


FIG. 1. (Color online) (a) LEED patterns for the clean W(110) substrate and the Fe thin films of different thicknesses on W(110). (b) The magnetic hysteresis loops measured by MOKE. The experiments are performed at room temperature except for the 1 ML Fe/W(110), which is measured at about 120 K.

20 and 30 meV. The degree of spin polarization P of the electron beam was 0.65 ± 0.08 . Energy resolved detection of outgoing electrons allows the determination of energy and in-plane momentum loss caused by the excitation of surface SWs. The spin of the incident electrons can be parallel either to the minority (down, \downarrow) or to the majority (up, \uparrow) electrons of the ferromagnetic samples, and so two intensity spectra, I_{\downarrow} and I_{\uparrow} , are obtained for the scattered electrons. A SW can be created only by the incidence of minority electrons due to the conservation of the angular momentum.¹¹ The SW peak is found in the I_{\downarrow} spectrum or, more clearly, in the difference $I_{\downarrow} - I_{\uparrow}$.

III. RESULTS AND DISCUSSION

The LEED patterns of the Fe films with different thicknesses are shown in Fig. 1(a). Sharp bcc (110) $p(1 \times 1)$ spots were observed on 1 ML Fe/W(110), which indicate the pseudomorphic growth of the first Fe layer on the W(110) substrate. The dislocation lines and dislocation networks start to appear subsequently in 2 ML and a bit thicker Fe films as proved by the appearance of satellite spots. To have a dislocation-free Fe surface a 20 ML Fe film was prepared and the sharp LEED spots represent a well-defined bcc (110) surface. The magnetic hysteresis loops of the Fe thin films measured by MOKE are shown in Fig. 1(b). The MOKE results indicate that all the Fe thin films are ferromagnetic with the easy axis of magnetization along the in-plane $[1\bar{1}0]$ direction. As the Curie temperature for 1 ML Fe/W(110) is about 220 K,²⁰ the MOKE and the later SPEELS measurements were performed at 120 K. The LEED and MOKE results show that the structural and magnetic properties of the Fe films are all consistent with the previous studies.^{21,22}

Figure 2 shows typical SPEEL spectra measured on 2 ML Fe/W(110) with the wave-vector transfer of 0.5 \AA^{-1} along the in-plane $[001]$ direction. Both the I_{\downarrow} and I_{\uparrow} spectra are

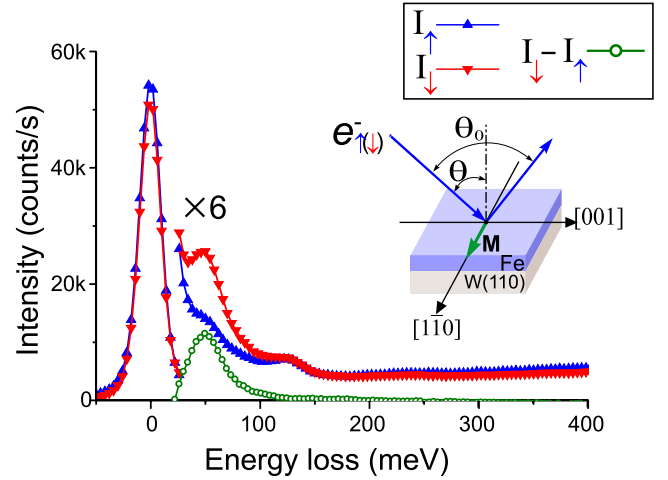


FIG. 2. (Color online) The SPEEL spectra measured with in-plane wave-vector transfer 0.5 \AA^{-1} . The up triangles (I_{\uparrow}) and down triangles (I_{\downarrow}) represent the intensity spectra of scattered electrons for the incidence of majority and minority electrons, respectively. The difference between the two spectra ($I_{\downarrow} - I_{\uparrow}$) is shown as circles. The scattering geometry is schematically illustrated in the inset. The spin wave is probed with the wave vector along the $[001]$ direction with the magnetization easy axis along the $[1\bar{1}0]$ direction. The incident energy of electrons is about 4 eV.

dominated by the quasielastic peak located at 0 meV energy loss. Since only minority electrons can create SWs in the sample, the inelastic peak due to the SW excitations can be easily distinguished at about 50 meV, where the excitations only create a pronounced peak in the I_{\downarrow} spectrum. One may also notice another excitation located at about 120 meV. It is attributed to the vibrational excitations due to the adsorption of hydrogen atoms at surface.²³ Since vibrational excitations are mediated by the Coulomb interaction, they are of nonspin-flip nature, which are evidenced by the almost identical peaks in both I_{\downarrow} and I_{\uparrow} spectra. It is more convenient to analyze the magnon peak in the difference spectrum defined as $I_{\downarrow} - I_{\uparrow}$, where the nonspin-flip excitations are almost canceled out. The scattering geometry is schematically illustrated in the inset. The in-plane momentum transfer is given by the scattering geometry $q = k_f \sin(\Theta_0 - \Theta) - k_i$, where k_i and k_f are, respectively, the magnitude of the wave vectors of the incident and scattered beams, Θ_0 is the angle between the incident beam and sample normal, and Θ is the angle between the incident and outgoing beams. In this work, Θ_0 is kept at 80° for all the measurements. Θ varies according to the desired surface wave-vector transfer.

Figure 3 presents SPEEL spectra measured for two in-plane momentum transfers 0.5 and 0.7 \AA^{-1} . A pronounced spin-dependent inelastic peak can be clearly seen at the energy loss about 40 meV, corresponding to the excitation of SWs. The SW energy changes nonmonotonously as the film thickness increases for both in-plane momentum transfers considered. SWs in 1 ML film have the lowest energy and experiences a sudden increase at 2 ML film. A local minimum is seen at about 4 ML and then the energy increases slightly in the thicker films. The asymptotic value of SWs energies is reached only at a relatively large coverage,

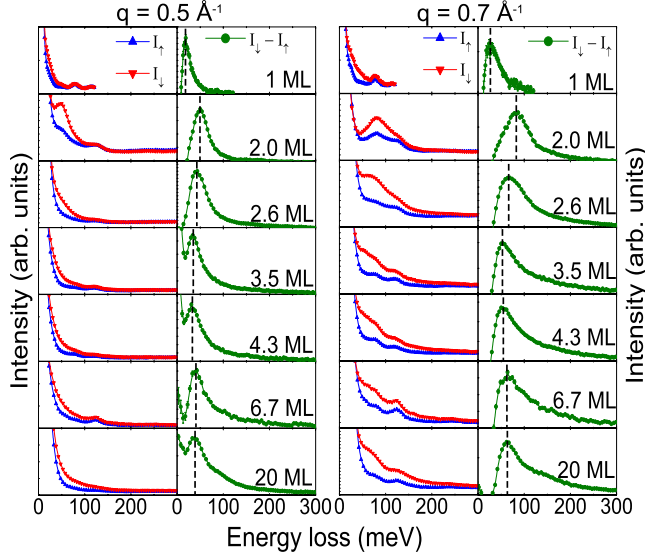


FIG. 3. (Color online) The SPEEL spectra, I_{\uparrow} and I_{\downarrow} measured for Fe films from 1 to 20 ML and the corresponding difference $I_{\downarrow} - I_{\uparrow}$. The wave-vector transfers are 0.5 \AA^{-1} (left) and 0.7 \AA^{-1} (right). The spectra for 1 ML are obtained at 120 K with incident energy of 3.8 eV. The other films are measured at room temperature using the incident energy of 4 eV. The energy resolution of the incident electron beam is about 20 meV.

around 7 ML. It should be noted that the Fe film thickness above 2 ML coverage is not uniform due to the statistical growth of Fe.¹¹ The spectrum contains excitations from patches of different thicknesses on the surface. Nevertheless, the tendency of the SW energies is clearly visible. For even higher wave vectors ($>0.7 \text{ \AA}^{-1}$), the trend is still preserved, however, due to broadening of the spectrum, the change is not clearly discerned as in the lower wave-vector case.

No straightforward physical argument exists to explain the observed nonmonotonous behavior. In the case of Co/Cu(100) films the SPEELS measurements could be interpreted by means of a nearest-neighbor Heisenberg model with the exchange integral taken from the bulk.¹³ A similar assumption for the Fe/W(110) system fails since it would result in $\omega_n(\mathbf{q}) = \omega_{\text{bulk}}(\mathbf{q})(2n-1)/2n$, i.e., $\omega_n(\mathbf{q})$ monotonously approaching the bulk value of SW energy from below.

To properly take into account the electronic structure of the film we performed first-principles adiabatic spin dynamics calculations based on density-functional theory (DFT). Within this approach the atomic magnetic moments are regarded as rigid entities precessing around the direction of the ground-state magnetization. The energies of the spin wave excitations are evaluated by means of parameter-free DFT calculations for the spiral magnetic structures with a given wave vector. This type of calculations allows also the mapping of the itinerant electron system onto a Heisenberg Hamiltonian¹⁷ and determination of the effective parameters of interatomic exchange interactions. We assume that the ground state is collinear with the magnetization pointing along the z direction. The direction of an atomic moment i is determined by two angles, see Fig. 4, panel U. The polar angle θ_i is the angle between the moment and the z axis and

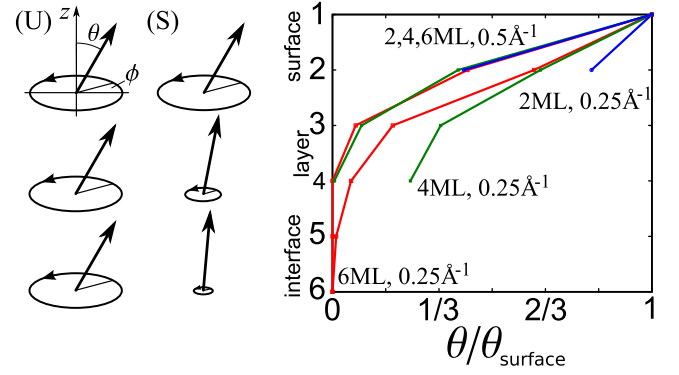


FIG. 4. (Color online) Angles θ_i of the surface mode for several selected coverages and momentum transfers; the values are normalized to the deviation in the uppermost layer taken to be 30 in the calculations. Above 0.5 \AA^{-1} all curves follow roughly one universal $\theta_i(\mathbf{q})$ dependence.

can be associated with the amplitude of a spin wave on a given atomic site. The azimuthal angle ϕ_i determines the phase of the moment in its precessional motion and is determined by the momentum of the spin wave, $\phi_i = \mathbf{q} \cdot \mathbf{s}_i$, where \mathbf{s}_i stands for the position of the i th atomic site. We estimate the SW energy $\omega(\mathbf{q})$ as the difference between the energy of the configuration of moments forming the SW, $E(\{\theta_i\}, \mathbf{q})$, and the ground-state energy E_0

$$\omega(\mathbf{q}) = \frac{2}{\Delta M} (E(\{\theta_i\}, \mathbf{q}) - E_0), \quad (1)$$

where $\Delta M = \sum_i (1 - \cos \theta_i) M_i$, M_i being the magnetic moment of the atom at site i . The normalization ensures that each SW changes the system magnetization by $2\mu_B$. We determine $E(\{\theta_i\}, \mathbf{q})$ using the spin-spiral technique.²⁴ It allows to find θ_i 's self-consistently: once a subset of angles is constrained to a specified value, the other angles are found ("relaxed") such that in the self-consistent state the spin-density matrices of the unrestricted sites are diagonal in the atomic coordinate systems.

The adiabatic spin dynamics neglects the presence of single-electron spin-flip excitations (Stoner excitations), therefore no prediction regarding the SWs' lifetimes can be made. However, the method provides a reliable account of the spin wave energies.²⁵

The small penetration depth of electrons in SPEELS experiment raises an important question about the spatial localization of the magnetic excitations measured in this experiment. Two limits can be considered: (1) the incoming electron excites mainly the uppermost (surface) magnetic moments while the dynamics of the deeper layers arises as a secondary effect due to the exchange coupling with the top layers or (2) the magnetic moments of all layers are equally involved in the excitation process and the spin wave mode is uniform with respect to the depth of the film. The present understanding of SPEELS does not allow us to make an *a priori* choice between these two scenarios. We perform a comparative study of both limits and relate the results of the calculations to the experimental data, focusing, in particular, on the maximum of the spin wave energy for the 2 ML film.

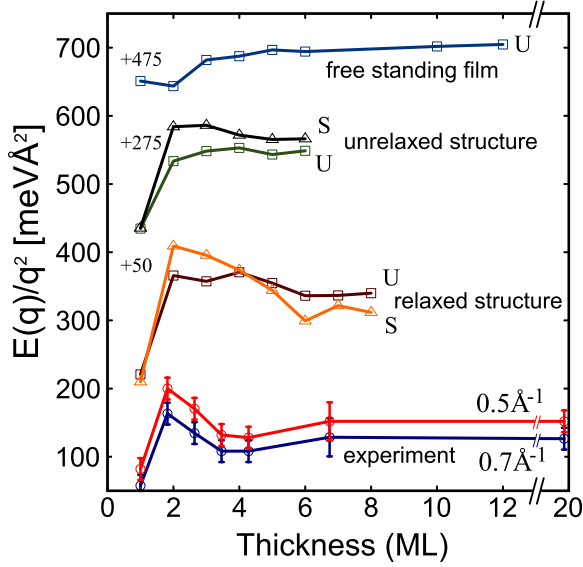


FIG. 5. (Color online) Energy of the SW modes (normalized to q^2) as a function of the film thickness; experimental results are compared to the theoretical calculations. Selected curves are shifted upward for the sake of improved clarity. The mode with the amplitudes (θ angles) of the moments forced to be equal in all film layers is marked with “U” (\square) while the surface mode bears symbol “S” (\triangle). All theoretical curves pertain to the momentum transfer of 0.5 \AA^{-1} .

The two limits are modeled as follows: in the uniform case the moments of all layers are restricted to deviate by the same angle θ . To simulate the excitation localized at the surface, only the angle θ of the moments of the surface layer is constrained whereas the directions of the moments of other layers are allowed to relax to self-consistent values.

We found that the relaxed magnetic configuration of the inner layers depends strongly on the wave vector of the SW. For $\mathbf{q}=\mathbf{0}$ we obtained the expected result that the moments of all layers deviate by the same angle θ as the constrained atomic moments of the surface layer, i.e., we obtained the collinear ferromagnetic structure rotated by the angle θ with respect to the original ground-state configuration. The uniformly rotated spin structure has exactly the same energy as the original one, which follows the Goldstone theorem stating that the energy of the $\mathbf{q}=\mathbf{0}$ SW must be zero in the absence of magnetic anisotropy, which we neglect. With increasing momentum transfer the deviation of the relaxed moments decreases with respect to the surface layer and with increasing depth of the layer, see Fig. 4. The degree of localization of the excitation also increases with decreasing the wavelength of the excitation.

First we performed calculations for the atomically unrelaxed films, characterized by the interlayer distances corresponding to the lattice parameter of bulk W. For both spin wave modes we get a strong increase in the excitation energy at the transition from 1 to 2 ML. For 1 ML film both modes are identical and have the same energy but for greater coverage they differ noticeably, Fig. 5. For the comparison with experiment it is important to note that the uniform mode does not have any maximum at 2 ML thickness. The energy

of this mode increases monotonously up to 4 ML and has a weak local minimum at 5 ML. On the other hand, the surface-type mode is much closer to the experimental behavior: the energies at 2 and 3 ML thicknesses are practically identical whereas they decrease noticeably starting from 4 ML. A possible reason for the less pronounced nonmonotonic behavior compared to experimental curves will be discussed below.

We now comment on the role of the substrate. We determined $\omega_n(\mathbf{q})$ dependence of the uniform mode for the free standing films. As seen in Fig. 5, the curve has a qualitatively different character than for the supported film. The energies for 1 and 2 ML are almost identical. From 2 to 3 ML the energy increases strongly and for greater coverage reaches monotonously the asymptotic value. This reveals the importance of the nonmagnetic W(110) substrate for the magnetic properties of the Fe film. The hybridization of the Fe and W states strongly influences the electronic structure of the film and in turn the exchange parameters and SW dispersion relation.²⁵

Returning to the supported films we took into account the atomic relaxations by using the interlayer distances determined experimentally.^{26,27} Accounting for atomic relaxation results in a significant change in the SW energy in Fig. 3. The surface-type mode is now very similar to the curve obtained in the experiment, with a clear maximum at the 2 ML thickness.

The remarkable difference of energies for 1 and 2 ML films has its origin in the interlayer exchange coupling, necessarily absent in the single monolayer film. (The interlayer exchange is defined as $J_{ll'}^0 = \sum_s J_{ls|s'0}$, where the Heisenberg exchange integral $J_{ls|s'}$ connects the moment s in the layer l with the moment s' in the layer l' .) The maximum of $\omega_n(\mathbf{q})$ observed at $n=2$ is the result of strong interlayer coupling $J_{12}^0 = 86.5 \text{ meV}$ in this system. We found that this fact seems to be a general property of Fe/W(110) films that the interlayer coupling is increased by 10–25 % between the two upper layers compared to pairs of deeper layers. This observation applies equally to the structurally unrelaxed and relaxed films. In the case of 2 ML coverage and structurally relaxed film the increase is particularly strong. Somewhat surprisingly the intralayer exchange energy, at least for the wave vectors considered, changes rather weakly with the thickness and the interlayer distances, so the variations in SW energies are mainly determined by the changes in $J_{ll'}^0$. The latter quantity reaches its minimum for the relaxed film at 6 ML coverage. Additionally, we note that the energy is generally smaller in the case of the unrelaxed film, where $J_{ll'}^0$ varies very weakly with the coverage reaching a value of around 61.0 meV for J_{12}^0 .

Although the calculated dependence of the SW energy on the film thickness agrees with experiment the theoretical energies are higher than measured ones.^{28,29} The unusual softening of the SW energies in Fe/W(110) films was noticed earlier and did not yet find its explanation. The account for Landau damping of the SW, because of the decay of the SW into Stoner excitations, can lead to the decrease in the SW energies, although the effect is not expected to be sufficient. Recently, it was shown that quantum corrections can lead to

the softening of the SW excitations.³⁰ These corrections are however strongly suppressed by the Hund's coupling. It remains an open question why the softening is observed for Fe films but is absent in the case of Co films.^{13,31} This important issue should be the topic of separate study.

IV. SUMMARY

In summary, we report a combined experimental and theoretical investigation of the SW excitations in thin Fe films grown on W(110). The experimental excitation energy shows nonmonotonous behavior with respect to the film thickness with a distinct maximum for 2 ML film. The results of the

density-functional theory calculations suggest that the SWs excited in the SPEELS experiment have an amplitude decaying with the depth of the layer. We demonstrate that accounting for the hybridization with the substrate and the atomic relaxation in the film is crucial for the theoretical description of the experiment.

ACKNOWLEDGMENTS

The authors thank A. Winkelmann for many interesting discussions. T.R.F.P. gratefully acknowledges the support of CNPq, Brazil. The authors also acknowledge the valuable discussions with D. L. Mills and R. Q. Wu.

*Corresponding author; wenxin.tang@sci.monash.edu.au

- ¹J. A. C. Bland and B. Heinrich, *Ultrathin Magnetic Structures: Fundamentals of Nanomagnetism* (Springer, New York, 2005).
- ²I. Žutić, J. Fabian, and S. Das Sarma, *Rev. Mod. Phys.* **76**, 323 (2004).
- ³D. J. Scalapino, *Phys. Rep.* **250**, 329 (1995).
- ⁴A. Hofmann, X. Y. Cui, J. Schäfer, S. Meyer, P. Höpfner, C. Blumenstein, M. Paul, L. Patthey, E. Rotenberg, J. Bünemann, F. Gebhard, T. Ohm, W. Weber, and R. Claessen, *Phys. Rev. Lett.* **102**, 187204 (2009).
- ⁵H. A. Mook and R. M. Nicklow, *Phys. Rev. B* **7**, 336 (1973).
- ⁶T. G. Perring, A. D. Taylor, and G. L. Squires, *Physica B* **213-214**, 348 (1995).
- ⁷B. Hillebrands, P. Baumgart, and G. Güntherodt, *Phys. Rev. B* **36**, 2450 (1987).
- ⁸T. Balashov, A. F. Takács, W. Wulfhekel, and J. Kirschner, *Phys. Rev. Lett.* **97**, 187201 (2006).
- ⁹C. L. Gao, A. Ernst, G. Fischer, W. Hergert, P. Bruno, W. Wulfhekel, and J. Kirschner, *Phys. Rev. Lett.* **101**, 167201 (2008).
- ¹⁰H. Ibach, D. Bruchmann, R. Vollmer, M. Etzkorn, P. S. Anil Kumar, and J. Kirschner, *Rev. Sci. Instrum.* **74**, 4089 (2003).
- ¹¹M. Plihal, D. L. Mills, and J. Kirschner, *Phys. Rev. Lett.* **82**, 2579 (1999).
- ¹²M. R. Vernoy and H. Hopster, *Phys. Rev. B* **68**, 132403 (2003).
- ¹³R. Vollmer, M. Etzkorn, P. S. Anil Kumar, H. Ibach, and J. Kirschner, *Phys. Rev. Lett.* **91**, 147201 (2003).
- ¹⁴W. X. Tang, Y. Zhang, I. Tudosa, J. Prokop, M. Etzkorn, and J. Kirschner, *Phys. Rev. Lett.* **99**, 087202 (2007).
- ¹⁵J. Prokop, W. X. Tang, Y. Zhang, I. Tudosa, T. R. F. Peixoto, K. Zakeri, and J. Kirschner, *Phys. Rev. Lett.* **102**, 177206 (2009).
- ¹⁶J. Hong and D. L. Mills, *Phys. Rev. B* **61**, R858 (2000).
- ¹⁷S. V. Halilov, H. Eschrig, A. Y. Perlov, and P. M. Oppeneer, *Phys. Rev. B* **58**, 293 (1998).
- ¹⁸A. T. Costa, R. B. Muniz, J. X. Cao, R. Q. Wu, and D. L. Mills, *Phys. Rev. B* **78**, 054439 (2008).
- ¹⁹R. Popescu, H. L. Meyerheim, D. Sander, J. Kirschner, P. Steadman, O. Robach, and S. Ferrer, *Phys. Rev. B* **68**, 155421 (2003).
- ²⁰M. Przybylski and U. Gradmann, *Phys. Rev. Lett.* **59**, 1152 (1987).
- ²¹X. Liu, M. M. Steiner, R. Sooryakumar, G. A. Prinz, R. F. C. Farrow, and G. Harp, *Phys. Rev. B* **53**, 12166 (1996).
- ²²K. Wagner, N. Weber, H. J. Elmers, and U. Gradmann, *J. Magn. Magn. Mater.* **167**, 21 (1997).
- ²³A. M. Baró and W. Erley, *Surf. Sci.* **112**, L759 (1981).
- ²⁴L. M. Sandratskii, *Adv. Phys.* **47**, 91 (1998).
- ²⁵P. Buczek, A. Ernst, L. Sandratskii, and P. Bruno, *J. Magn. Magn. Mater.* **322**, 1396 (2010).
- ²⁶H. L. Meyerheim, D. Sander, R. Popescu, J. Kirschner, P. Steadman, and S. Ferrer, *Phys. Rev. B* **64**, 045414 (2001).
- ²⁷D. Sander, R. Skomski, C. Schmidthals, A. Enders, and J. Kirschner, *Phys. Rev. Lett.* **77**, 2566 (1996).
- ²⁸Y. Zhang, Ph.D. thesis, Martin-Luther University, 2009.
- ²⁹L. Udvardi and L. Szunyogh, *Phys. Rev. Lett.* **102**, 207204 (2009).
- ³⁰S. Pandey and A. Singh, *Phys. Rev. B* **78**, 014414 (2008).
- ³¹M. Etzkorn, P. S. Anil Kumar, W. Tang, Y. Zhang, and J. Kirschner, *Phys. Rev. B* **72**, 184420 (2005).